Journal of Radioanalytical and Nuclear Chemistry (2024) 333:1991–1998
https://doi.org/10.1007/s10967-024-09420-x

Pertechnetate removal from aqueous solutions by chitosan/hydroxyapatite composites

Lucia Hagara Pivarčiová[1] · Oľga Rosskopfová[1] · Marek Hupian[1] · Eva Viglašová[1] · Michal Galambošš[1] · Dominik Juračka[1] · Pavol Rajec[1,2]

Received: 9 November 2023 / Accepted: 7 February 2024 / Published online: 7 March 2024

Abstract
This study focuses on the usage of chitosan/hydroxyapatite composites for pertechnetate removal from aqueous solutions. Pertechnetate, a prominent radionuclide in nuclear waste, presents environmental hazards due to its long half-life and mobility. The composites, formed by intergrating hydroxyapatite into chitosan matrices, demonstrate in situ nanohydroxyapatite generation. Investigation of the adsorption process involves assessing parameters like pH, contact time, and the influence of competetive ions. This research provides valuable insights for using composites to mitigate pertechnetate contamination.

Keywords Chitosan · Hydroxyapatite · Composites · Pertechnetate · Adsorption

Introduction

Technetium-99 is a fission product of uranium, constituting approximately 6.06% of its yield. Sources of technetium release into the environment include nuclear power plants [1], spontaneous fission or cosmic radiation reactions [2], medical applications [1] nuclear accidents, nuclear weapon tests [3] and nuclear fuel reprocessing [4]. Its long half-life (nearly 211,000 years) and the mobility of its most abundant chemical form, pertechnetate, make its determination crucial to assess the potential environmental impact [5]. The persistence of its activity in radioactive waste poses a threat even after thousands of years, necessitating effective control measures. Recent reasearch has focused on understanding the biogeochemical behaviour of technetium, its pathways in food chains, and developing methods to control its mobility in various systems [6]. Conventional methods for radionuclide and heavy metal removal from aqueous soulutions, including precipitation, ion-exchange, extraction chromatography, and adsorption, have been explored. Adsorption, due to its simplicity and the variability of adsorbent materials, is considered one of the most suitable methods for this application [7]. Multiple adsorbents, such as clay minerals, activated carbons, biochars, tin-based materials, organic adsorbents, and biopolymers, have been tested for their efficiency in technetium removal [8]. Chitosan and hydroxyapatite had been previously tested for pertechnetate, and other heavy metal ions adsorption. However, the usage of their composites have not been yet explored for this application [6, 9–12].

Hydroxyapatite ($Ca_{10}(PO_4)_6(OH)_2$ is naturally present in phosphate rocks (60–70%), and it is a component of biomaterials such as bones, teeth, and milk. Due to its exceptional qualities, hydroxyapatite stands out as a predominant biomaterial for hard tissue regeneration [13–16]. Its wide-ranging applications include dental implants, biodegradable scaffolds, and orthopedic implants. Notably, hydroxyapatite's chemical similarity to bone and compatibility with various polymers contribute to its effectiveness. Its role extends to adsorbing heavy metals and radionuclides, owing to its low solubility and remarkable properties [17–22].

Chitosan, derived from chitin, exhibits rigidity and finds application in bone growth enhancement, such as in bone-filling paste [23–25]. Despite insolubility in neutral pH, it forms water-soluble salts with acids. Controlled deacetylation and depolymerization processes alter its characteristics. Chitosan's diverse properties, including non-toxicity, biocompatibility, and bioactivity, make it attractive for pharmaceutical and medical applications [26, 27]. Its utility extends

✉ Marek Hupian
marek.hupian@uniba.sk

[1] Department of Nuclear Chemistry, Faculty of Natural Sciences, Comenius University Bratislava, Mlynská Dolina Ilkovičova 6, 842 15 Bratislava, Slovak Republic

[2] BIONT a.s., Karloveská 63, 842 29 Bratislava, Slovak Republic

to bone tissue engineering, implants, and various sectors beyond healthcare [28, 29]. In tissue engineering, transient scaffolds play a crucial role in supporting tissue growth and repair. Chitosan scaffolds, mirroring glycosaminoglycans, offer an excellent substrate for cell growth and proliferation. Their commendable osteoconductivity enhances bone formation in both laboratory and living organism conditions [30]. Conventional chitosan/hydroxyapatite composite preparation involves mixing particles under controlled conditions [31, 32]. However, uneven distribution and nanoparticle agglomeration pose challenges. An alternative in-situ generation method anticipates more consistent structures, addressing aggregation issues and enhancing clinical performance [33–36].

This paper introduces two unique approaches to prepare chitosan/hydroxyapatite composites. The first involves mixing particles with chitosan matrices, while the second centers on in-situ nanohydroxyapatite generation within the chitosan matrix. Our research is then focused on adsorption capability of these materials for pertechnetate adsorption for the very first time. The examined parameters influencing the adsorption process are pH of the solution, contact time, and the presence of competetive ions.

Materials and methods

Reagents

All chemicals, that were used in this study, were sourced from reputable suppliers. Specifically, analytical reagent-grade pure materials were produced from Slavus, s.r.o., Bratislava, Slovak Republic, and Lachema n.p., Brno, Czech Republic. The chitosan, characterized by medium molecular weight and a deacetylation degree of 75–85%, was acquired from Sigma-Aldrich, Germany. A synthetic hydroxyapatite, of puriss grade, was obtained from Sigma-Aldrich Chemie GmbH, Germany. In addition, pertechnetate in the form of $^{99m}TcO_4^-$ was used as a radioindicator and was obtained by elution from $^{99}Mo/^{99m}Tc$ generator DRYTEC (with activity range of 2.5–100 GBq), manufactured by GE Healthcare, available at 1200 GMT.

Preparation and characterization of the chitosan/hydroxyapatite composites

CH/HA(A), CH/HA(B) composite

Chitosan solution with the analytical concentration of 6% (w/v) was prepared by dissolving chitosan in 2% (v/v) acetic acid and stirring for 24 h to get a completely transparent solution. Subsequently, the solution was mixed with phosphoric acid and the ethanol solution of calcium hydroxide with the analytical concentration of 8.20% (v/v) and 10.33% (v/v), respectively. The mixture was then stirred for 24 h, and then pH was adjusted to 5.5 with the solution of 3% (v/v) acetic acid to obtain a gelatinous mixture of chitosan/hydroxyapatite. 50% aqueous solution of glutaraldehyde was added to the gel of CH/HA(A) and CH/HA(B) with the final glutaraldehyde amount in solution of 0.022 mol and 0.011 mol, respectively. The mixture was stirred for 1 h at room temperature. The precipitate was filtered, and washed with distilled water to remove any unreacted glutaraldehyde. Finally, the precipitate was washed with 1 M hydrochloric acid solution to remove a non-crosslinking chitosan, 0.2 M sodium hydroxide solution, distilled water, and acetone. The precipitate was dried at room temperature. The weight ratio of the prepared CH/HA composite was 30:70 [34, 37].

CH/HA composites with different weight ratio (30:70, 50:50, 100:0)

Chitosan solutions with different analytical concentrations were prepared by dissolving chitosan in 2% (v/v) acetic acid, and stirring for 3 h to get a completely transparent solution. Subsequently, the solution was mixed with hydroxyapatite, and stirred for 2 h and then pH was adjusted to 5.5 with the solution of 0.2 M sodium hydroxide solution to obtain a gelatinous mixture of chitosan/hydroxyapatite. 50% aqueous solution of glutaraldehyde was added to the gel of CH/HA with the final glutaraldehyde concentration of 87.5 mmol per 1 g of chitosan. The mixture was then stirred for 1 h at room temperature. The precipitate was filtered, and washed with distilled water to remove any unreacted glutaraldehyde. Finally, the precipitate was washed with 1 M hydrochloric acid solution to remove a non-crosslinking chitosan, 0.2 M sodium hydroxide solution, distilled water, and acetone. The precipitate was dried at room temperature [30, 34]. The composites CH/HA with different weight ratio composition of chitosan and hydroxyapatite are listed in Table 1.

Multiple characterization methods were used to study the samples. The morphology and the particle size of the samples of chitosan/hydroxyapatite composites CH/HA(A), CH/HA(B), CH/HA 30:70, CH/HA 50:50 and CH/HA 100:0 were examined using a scanning electron microscope, type JOEL JX-84A (SEM). The specific surface area value of the composite samples with different CH/HA ratios was

Table 1 Preparation of chitosan/hydroxyapatite composites

Sample	CH/HA composition (weight ratio)	Chitosan (g)	Hydroxyapatite (g)
CH/HA 30:70	30/70	0.18	0.42
CH/HA 50:50	50/50	0.30	0.30
CH/HA 100:0	100/0	0.60	0.00

determined with BET isotherm analysis (physical adsorption of nitrogen technique). The presence and quality of functional groups on the sample´s surface was verified via Fourier-transform infrared spectroscopy (FTIR), using spectrometer NICOLET 6700.

Adsorption experiments

For the adsorption of pertechnetate on chitosan/hydroxyapatite composites, methodology for the experiments was adopted from our prior research [9–12]. As a radioindicator, ^{99m}Tc in the form of $^{99m}TcO_4^-$was used. A batch method was used in static arrangement of experiments under aerobic conditions at laboratory temperature, without usage of a carrier solution. Adsorption parameters were determined after adding 3 mL of aqueous phase to 30 mg of sorbent in a plastic tube (1:100 ratio) with tap and both phases were mixed in lab rotator with constant speed of mixing 30 rpm. After adsorption of pertechnetate, the suspension was centrifugated at 6000 rpm for 10 min and an adequate aliquot of the supernatant was measured on the gamma counter 1470 Wizard using NaI(Tl) detector. The relative error of the measurement was below 1%.

The influence of contact time on the technetium adsorption was analyzed from 1 up to 3 h. The equilibrium time for further experiments was chosen to be 1 h.

Adsorption behaviour of pertechnetate was studied as a function of pH. The initial solution consisted of distilled water with pH values that were adjusted from ~ 3 to ~ 10, using HCl or NaOH solutions and labelled with ^{99m}Tc, without using a carrier. The pH measurements were performed using pH meter CPH 51 from Fisher Scientific Co. before the experiment (initial pH_i) and after the interaction of sorbent with the solution at the equilibrium time (final pH_f).

Effect of different ions presented in the solution on the adsorption of pertechnetate was studied using various cations with the analytical concentration: 1×10^{-2} mol dm^{-3} and anions in the analytical range of 1×10^{-4}–1×10^{-1} mol dm^{-3}. The solutions of the cations were prepared from their chloride salt and distilled water.

Adsorption properties of the adsorbent were calculated using the following equations:

- Distribution coefficient K_D:

$$K_D = \frac{c_0 - c_{eq}}{c_{eq}} \cdot \frac{V}{m} = \frac{a_0 - a}{a} \cdot \frac{V}{m} \left[\mathrm{cm^3 \cdot g^{-1}}\right]$$

- Adsorption percentage R:

$$R = \frac{100 \cdot K_D}{K_D + \frac{V}{m}} [\%]$$

where c_0 is initial analytical concentration of the adsorbate (mol dm^{-3}), c_{eq} is equilibrium concentration of the adsorbate (mol dm^{-3}), V is volume of aqueous phase (cm^3), m is mass of sorbent (g), a_0 is volume activity of the initial solution (Bq cm^{-3}) and a is equilibrium volume activity of the solution (Bq cm^{-3}).

Results and discussion

The size and form of CH/HA composites were determined by scanning electron microscopy (SEM). Figure 1 illustrates the scanning electron micrographs of the chosen composites, showing a variety of forms and size of the particles. The difference in morphology between these composites can be attributed to the different preparation of composites and the different weight ratio of chitosan to hydroxyapatite in the composite. CH/HA(A) with the weight ratio of 30:70 was prepared mixing the hydroxyapatite particles with chitosan matrices. The size of irregular shapes was 50–100 µm (Fig. 1A). The SEM of CH/HA(A) composite at a higher magnification is presented in Fig. 1B. The scanning elector micrographs of CH/HA 50:50 composite prepared with method by in-situ generation of nanohydroxyapatite in the chitosan matrix show the polymer structure of this composite (Fig. 1C). The increasing of the amount of chitosan in the composite increased its polymeric properties. SEM of CH/HA 50:50 composite at a higher magnification is presented in Fig. 1D. Other composites prepared with the same method had similar the morphology and the particle size.

The specific surface area values of the CH/HA composites with different CH/HA ratios are summarized in Table 2. This provides insights into the composite´s structural characteristics, influencing its adsorption capacity. Higher specific surface area values generally correlate with increased available binding sites for adsorption processes; hence, is should have higher adsorption capacity. By tailoring the composite´s composition, we can potentially enhance its adsorption performance and overall effectiveness in adsorption applications. Clearly, the more addition of hydroxyapatite to the composite, the bigger S_{BET} value. This is due to the higher specific surface area value of the hydroxyapatite itself ($S_{BET} = 52.8$ m^2 g^{-1}).

The FTIR spectra presented in Fig. 2 showcase the functional groups in CH/HA composites. In the spectrum of pure CH (composite CH/HA ratio 100:0), a broad peak at 3440 cm^{-1} corresponds to the hydroxyl group of chitosan. The bands at around 1650–1600 cm^{-1} correspond to the =C=O stretching vibrations and =N–H, characteristic of amide structures. The peak at 1255 cm^{-1} of the amide structure diminishes with increasing hydroxyapatite content in the composite samples. When comparing between compsites, significant changes can be observed. The intensity of

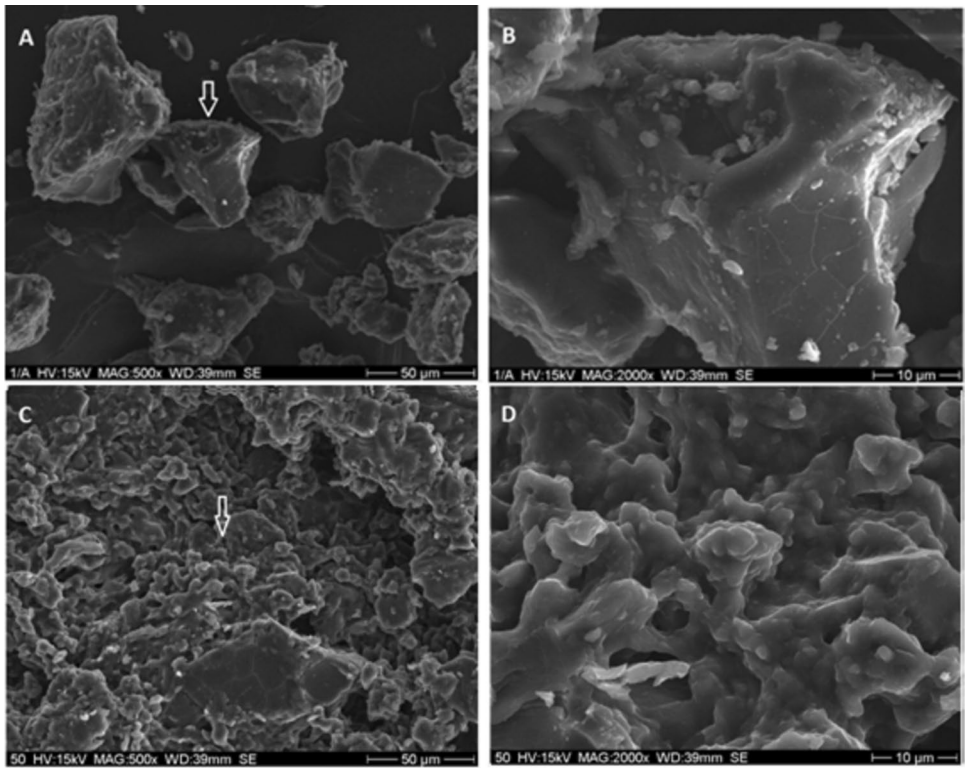

Fig. 1 Electronmicroscopic image of chitosan/hydroxyapatite composites **A,B** CH/HA (A); **C, D** CH/HA 50:50

Table 2 Specific surface area values for CH/HA composite samples

Sample	CH/HA composition (weight ratio)	S_{BET} value ($m^2\ g^{-1}$)
CH/HA 30:70	30/70	37,32
CH/HA 50:50	50/50	26,86
CH/HA 100:0	100/0	1,20

the –CH vibrations belonging to chitosan decreases with increasing hydroxyapatite content in the sample. Hydrogen interactions between CH and HA can be confirmed with a peak at 895 cm^{-1}. Peaks related to hydroxyl group stretching vibrations show a slight shift towards lower wavenumbers in the composites, indicative of hydrogen bond formation between mineral and biopolymer compounds.

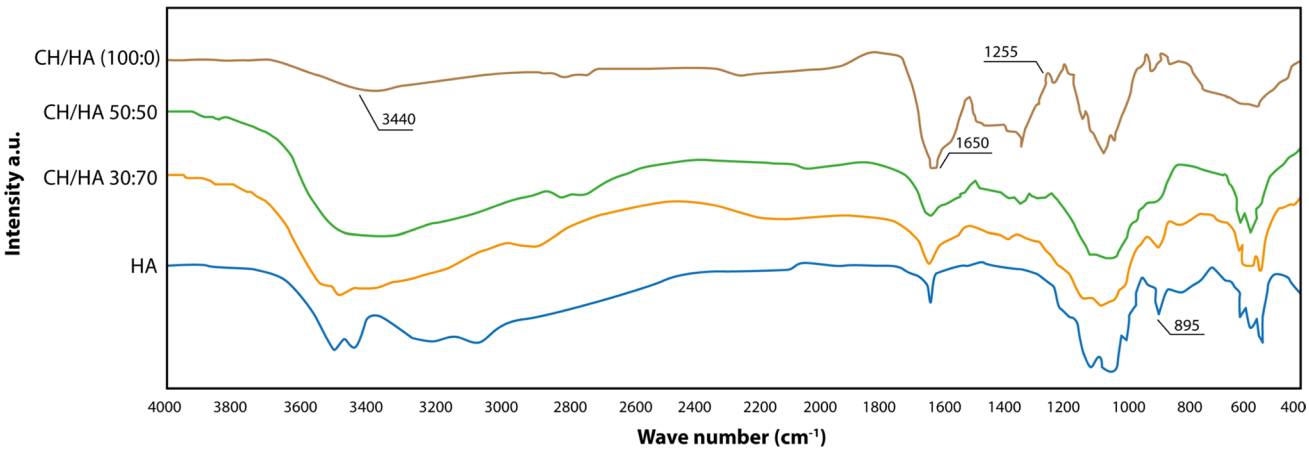

Fig. 2 FTIR spectra of CH/HA composites

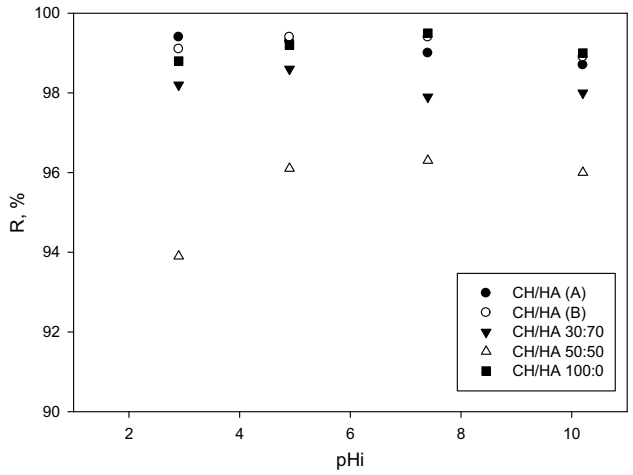

Fig. 3 Influence of initial pH on the adsorption of pertechnetate using CH/HA samples (contact time: 1 h, without carrier)

Table 3 Results of adsorption experiments: adsorption percentage, initial pH and final pH

Samples	R%				
	pH_i	2.9	4.9	7.4	10.2
	pH_f				
CH/HA (A)	5.5	99.4	99.3	99.0	98.7
CH/HA (B)	4.0	99.1	99.4	99.4	98.9
CH/HA 30:70	4.0	98.2	98.6	97.9	98.0
CH/HA 50:50	3.5	93.9	96.1	96.3	96.0
CH/HA 100:0	4.0	98.8	99.2	99.5	99.0

The adsorption mechanism of pertechnetate onto CH/HA composites consists of various partial mechanisms, each providing a different aspect of the interaction. The amino groups in chitosan engage in ion exchange, while surface complexation and electrostatic attraction occus at the hydroxyapatite surface. Additionally, hydrogen bonding with chitosan´s hydroxyl groups contributes to the process. The formation of nanohydroxyapatite within the chitosan matrix creates more favourable adsorption sites for the anion. Our experimental analyses (FTIR, SEM) provide support to these proposed mechanisms.

The influence of contact time of the aqueous and solid phase was investigated in the range from 1 to 3 h on the chitosan/hydroxyapatite composites. The total adsorption of pertechnetate did not change remarkably after 1 h, therefore we´ve chosen 1 h to be suitable for further batch experiments. The adsorption percentage of pertechnetate onto composites was > 97%.

During the adsorption process, the pH value is generally the key parameter, since it controls not only the surface charge of an adsorbent, but also metal speciation. Figure 3 and Table 3 shows the effect of initial pH on the adsorption percentage. On the initial pH range of 2.9–10.2, the adsorption percentage of pertechnetate on chitosan/hydroxyapatite composites was > 94%, due to the presence of amino and hydroxyl functional groups on chitosan, and excellent buffering properties of the synthetic hydroxyapatite. It is clear that the removal efficiency was approximately same, because the pH value after the equilibrium was reached, was nearly the same for all of the investigated CH/HA composites. Measured pH after the adsorption was in the range of 3.5–5.5.

The influence of different, potentially competitive cations Na^+, Cs^+, NH_4^+, Ca^{2+}, Co^{2+}, Fe^{2+}, Fe^{3+} were observed in regard to pertechnetate adsorption on the CH/HA 100:0, CH/HA 50:50 and CH/HA 30:70 composites at analytical concentration of 1×10^{-2} mol dm^{-3}. The highest adsorption percentage was achieved on crosslinked chitosan. The presence of different ions in solution had no effect on the adsorption of pertechnetate on CH/HA 100:0. The competitive effect of Fe^{2+} and Fe^{3+} cations towards $^{99m}TcO_4^-$ adsorption was stronger than other ions on CH/HA 30:70 and CH/HA 50:50 composites. The adsorption percentage of pertechnetate on CH/HA 100:0, CH/HA 50:50 and CH/HA 30:70 composites in the presence of different ions in solution with concentration of 1×10^{-2} mol dm^{-3} is presented in Fig. 4A.

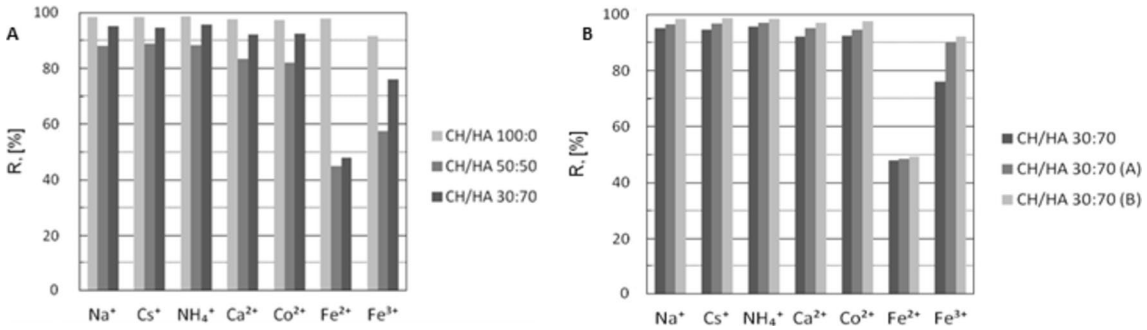

Fig. 4 Influence of presence of different cations on adsorption percentage of pertechnetate on CH/HA composites; **A** CH/HA with different weight ratio; **B** CH/HA with different preparation method

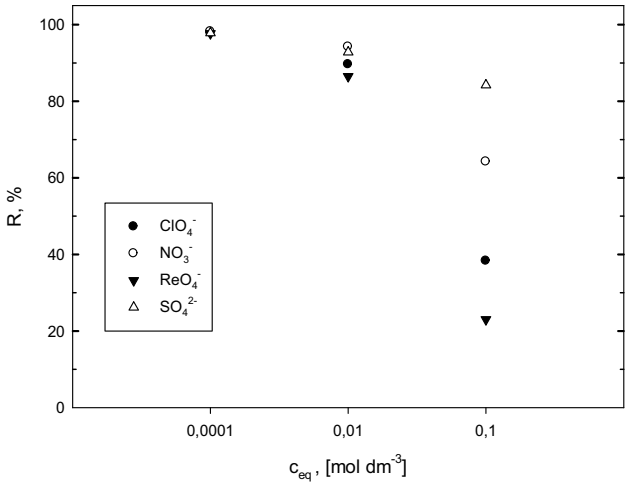

Fig. 5 Influence of presence of different anions on adsorption percentage of pertechnetate on CH/HA composite 50:50

The influence of different cations Na^+, Cs^+, NH_4^+, Ca^{2+}, Co^{2+}, Fe^{2+}, Fe^{3+} on the pertechnetate adsorption was investigated on CH/HA 30:70, CH/HA(A), CH/HA(B) composites at concentration of 1×10^{-2} mol dm^{-3} (Fig. 4B). Adsorption percentage of pertechnetate was the same for all of the composites with the weight ratio of 30:70. The effect of Fe^{2+} towards TcO_4^- adsorption was stronger than the competition effect of other observed cations for all examined composites with the same weight ratio. Ferrous cations can cause the reduction of pertechnetate to lower oxidation state in the composite containing the hydroxyapatite, thus reducing the adsorption percentage, or adsorption capacity [9, 38, 39].

The effect of different anions on the technetium adsorption was studied using the solutions of anions in analytical concentration of 1×10^{-4}–1×10^{-1} mol dm^{-3}. The influence of NO_3^-, ClO_4^-, ReO_4^- and SO_4^{2-} on the adsorption of technetium on all of studied CH/HA composites was investigated (Fig. 5).

The adsorption percentage of pertechnetate on composite CH/HA 50:50 in the presence of different anions decreased in following order: $ReO_4^- > ClO_4^- > NO_3^- > SO_4^{2-}$. In the case of other studied composites, the adsorption was nearly the same. The competitive effect of ReO_4^- towards TcO_4^- adsorption was stronger than the competition effect of other observed anions, due to perrehenate being a chemical analogue to pertechnetate. Perrehenate is also being used as a carrier for pertechnetate (technetium) in radiochemical analyses. Liu et al. studied the removal od fluoride from aqueous solution Zr(IV) immobilized cross-linked chitosan. They investigated effect of the presence of different anions on adsorption. The presence of these anions presented negative effect on the removal efficiency of fluoride. The adsorption was decreased in the order $Cl^- > SO_4^{2-} > CO_3^{2-} > PO_4^{3-}$. A decrease in the adsorption of fluoride in the presence of Cl^- and SO_4^{2-} ions may occur due to the competition among the anions for the sites on the adsorbent surface [40].

Conclusions

In the present study, chitosan/hydroxyapatite composites were synthesized through two distinct methodologies. The first approach involved the mixing of hydroxyapatite particles with chitosan matrices, while the second method entailed the in-situ generation of nanohydroxyapatite within the chitosan matrix. The samples were characterized via SEM, BET and FTIR characterization methods, which confirmed the successful preparation of the samples and the presence of the functional groups important for pertechnetate adsorption. The utility of these composites for the removal of pertechnetate anions from aqueous solutions was examined using batch adsorption technique, under static experimental conditions conducted at ambient laboratory temperature. The effect of contact time of the phases, initial pH and presence of different, potentially competitive ions regarding pertechnetate adsorption onto these materials was investigated. Adsorption percentage of pertechnetate reached 97% after just 1 h of contact time of the phases. In the initial pH range spanning from 2.9 to 10.2, the adsorption of pertechnetate on chitosan/hydroxyapatite composites consistently surpassed 94%. Furthermore, the competitive effect of Fe^{2+} ions on pertechnetate adosprtion exhibited greater potency compared to other observed cations across all examined composites. Similarly, the competitive influence of ReO_4^- anions on pertechnetate adsorption exceeded that of other observed anions. These findings suggest, that the adsorption mechanisms are likely governed by ion exchange processes. In summary, the chitosan/hydroxyapatite composited investigated in this study hold promise as potential alternative adsorbents for effectively removing $^{99m}TcO_4^-$ from aqueous solutions.

Acknowledgements This study was supported by the Operation Program of Integrated Infrastructure for the project, UpScale of Comenius University Capacities and Competence in Research, Development and Innovation, ITMS2014+: 313021BUZ3, and Agency of the Ministry of Education, Science, Research and Sport of the Slovak Republic and Slovak Academy of Sciences VEGA Project No. 1/0356/23.

Funding Open access funding provided by The Ministry of Education, Science, Research and Sport of the Slovak Republic in cooperation with Centre for Scientific and Technical Information of the Slovak Republic.

Data availability All data generated or analysed during this study are included in this published article.

Declarations

Conflict of interest The autors declare that they have no conflict of interest.

References

1. Shi K, Hou X, Roos P, Wu W (2012) Determination of technetium-99 in environmental samples: a review. Anal Chim Acta 709:1–20
2. Schulte EH, Scoppa P (1987) Sources and behaviour of technetium in the environment. Sci Total Environ 64(1–2):163–179
3. Aarkrog A, Dahlgaard H, Hallstadius L, Holm E, Mattsson S, Rioseco J (1986) Time trend of 99Tc in seaweed from greenland waters. In: Desmet G, Myttenaere C (eds) Technetium in the Environment. Springer, Dordrecht
4. Meena AH, Arai Y (2017) Environmental geochemistry of technetium. Environ Chem Lett 15:241–263
5. Lehto J, Hou X (2011) Chemistry and analysis of radionuclides: laboratory techniques and methodology. Wiley and Sons, Hoboken
6. Rosskopfová O, Viglašová E, Galamboš M, Daňo M, Tóthová D (2023) The removal of pertechnetate from aqueous solution by synthetic hydroxyapatite: the role of reduction reagents and organic ligands. Int J Environ Res Public Health 20(4):3227
7. Chmielewska E, Bujdoš M, Hupian M, Galamboš M (2023) Kinetic and isotherm studies for Cu^{2+} and Cs^{+} uptake with mono- and biometallic FeO(OH)-MnOx-clinoptilolite. Minerals 13:1536
8. Wang J, Xu B (2023) Removal of radionuclide 99Tc from aqueous solution by various adsorbents: a review. J Environ Radioact 270:107267
9. Rosskopfová O, Galamboš M, Pivarčiová L, Čaplovičová M, Rajec P (2013) Adsorption of nickel on synthetic hydroxyapatite from aqueous solutions. J Radioanal Nucl Chem 295:459–465
10. Pivarčiová L, Rosskopfová O, Galamboš M, Rajec P (2014) Adsorption behaviour of Zn(II) ions on synthetic hydroxyapatite. Desalin Water Treat 7:1825–1831
11. Pivarčiová L, Rosskopfová O, Galamboš M, Rajec P (2014) Sorption of nickel on chitosan. J Radioanal Nucl Chem 300:361–366
12. Pivarčiová L, Rosskopfová O, Galamboš M, Rajec P, Hudec P (2016) Sorption of pertechnetate anions on chitosan. J Radioanal Nucl Chem 308:93–98
13. Combes C, Rey C (2010) Amorphous calcium phosphates: Synthesis, properties and uses in biomaterials review. Acta Biomater 6:3362–3378
14. Dorozhkin SV (2009) Nanodimensional and nanocrystalline apatites and othes calcium orthophosphazes in biomedical engineering, biology and medicine review. Mater 2:1975–2045
15. Kwon SH, Jun YK, Hong SH, Kim HE (2003) Synthetis and sissolution behavior of β-TCP and HA/β-TCP composite powder. J Eur Ceram Soc 23:1039–1045
16. Sjoberg S, Bengtsson A (2009) Surface complexation and proton promoted dissolution in aqueous apatite systems. Geochmica et Cosmochimica Acta 73(9):1233–1584
17. Handley-Sidhu S, Renshaw JC, Yong P, Kerley R, Macaskie LE (2011) Nano-crystalline hydroxyapatite bio-mineral for treatment of strontium from aqeous solutions. Biotechnol Lett 33:79–87
18. Tripathi A, Saravanan S, Pattnaik S, Moorthi A, Partridge NC, Selvamurugan N (2012) Bio-composite scaffolds containing chitosan/nano-hydroxyapatite/nano-coper-zinc for bone tissue engineering. Int J Biol Macromol 50:294–299
19. Elouear Z, Bouzid J, Boujelben N, Feki M, Jamoussi F, Montiel A (2008) Heavy metal removal from aqueous solutions by activated phosphate rock. J Hazard Mater 156:412–420
20. Geshalaev SV, Demirchan CA (2012) Synthsis, properties and applications of hydroxyapatite, 1st edn. Nova Science Publishers Inc, New York, pp 1–491 (**ISBN: 978-1-62081-934-0**)
21. Galamboš M, Suchánek P, Rosskopfová O (2013) Sorption of anthropogenic radionuclides on natural and synthetic inorganic sorbents. J Radioanal Nucl Chem 293:613–633
22. Mucalo M (2015) Hydroxyapatite (HAp) for biomedical applications, 1st edn. Woodhead Publishing Elsevier, England, pp 1–387 (**ISBN 978-1-78242-033-0**)
23. Ibrahim MA, Alhalafi MH, Emam EAM, Ibrahim H, Mosaad RH (2023) A review of chiosan and chitosan nanofiber: preparation, characterization, and its potential applications. Polymers 15:2820
24. Solovtsova OV, Grankina TYu, Krasil'nikova OK, Serebryakova NV, Shinkarev SM, Voloshchuk AM (2008) The effect of the dehydration conditions of chitosan-based polymeric adsorbents on the adsorption of nickel cations. J Colloid 70:341–348
25. Swayampakula K, Boddu VM, Nadavala SK, Abburi K (2009) Competitive adsorption of Cu (II), Co (II) and Ni (II) from their binary and tertiary aqeous solutions using chitosan-coated perlite beads as biosorbent. J Hazard Mater 170:680–689
26. Miretzky P (2009) Hg (II) removal from water by chitosan and chitosan derivates: a review. J Hazard Mater 167:10–23
27. Mourya VK, Inamdar NN (2008) Chitosan-modifications and applications: opportunities galore. React Funct Polym 68:1013–1051
28. Qiu Y, U C (2008) Chitosan derivates for tissue engineering, Clemsom University.
29. Madni A, Kousar R, Naeem N, Wahid F (2021) Recent advancements in applications of chitosan-based biomaterials for skin tissue engineering. J Bioresour Bioprod 6:11–25
30. Chen Y, Wang J (2012) Removal of radionuclide Sr2+ ions from aqueous solution using synthesized magnetic chitosan beads. Nucl Eng Des 242:445–451
31. Sivakumar M, Manjubala I, Rao KP (2002) Preparation, characterization and in-vitro release of gentamicin from coralline hydroxyapatite–chitosan composite microspheres. Carbohydr Polym 49:281–288
32. Granja PL, Silva AIN, Borges JP, Barrias CC, Amaral IF (2004) Preparation and characterization of injectable chitosan-hydroxyapatite microspheres. Key Eng Mater 254–256:573–576
33. Ding C, Teng S, Pan H (2012) In-situ generation of chitosan/hydroxyapatite composite microspheres for biomedical application. Mater Lett 79:72–74
34. Mohamed KR, El-Rashidy ZM, Salama AA (2011) In vitro properties of nano-hydroxyapatite/chitosan biocomposites. Ceram Int 37:3265–3271
35. Pighinelli L (2013) Chitosan–hydroxyapatite composites. Carbohyd Polym 93:256–262

36. Chesnutt BM, Yuan Y, Buddington K, Haggard WO, Bumgardner JD (2009) Composite chitosan/nano-hydroxyapatite scaffolds induce osteocalcin production by osteoblasts in vitro and support bone formation in vivo. Tissue Eng A 15:2571–2579
37. Chen A, Yang Ch, Chen Ch (2009) The chemically crosslinked metal-complexed chitosans for comparative adsorptions of Cu (II), Zn (II), Ni (II) and Pb (II) ions in aqueous medium. J Hazard Mater 163:1068–1075
38. Peretyazhko TS, Zachara JM, Kukkadapu RK, Heald SM, Kutnyakov IV, Resch CT, Arey BW, Wang CM, Kovarik L, Philips JL, Moore DA (2012) Pertechnetate (TcO4-) reduction by reactive ferrous iron forms innaturally anoxic, redox transition zone sediments from the hanford site, USA. Geochim Cosmochim Acta 92:48–66
39. Kohlíčková M, Jedináková-Křížová V, Melichar F (1998) Technetium Complexes—their possible use in radiopharmacy and pharmacokinetic properties. Chem Listy 92:643–655
40. Liu Q, Zhang L, Yang B, Huang R (2015) Removal of fluoride from aueous solution using Zr(IV) immobilized cross-linked chitosan. Int J Biol Macromol 77:15–23